Article

Modified Active Site Coordination in a Clinical Mutant of Sulfite Oxidase

Christian J. Doonan, Heather L. Wilson, K. V. Rajagopalan, Robert M. Garrett, Brian Bennett, Roger C. Prince, and Graham N. George

J. Am. Chem. Soc., **2007**, 129 (30), 9421-9428• DOI: 10.1021/ja071402a • Publication Date (Web): 04 July 2007

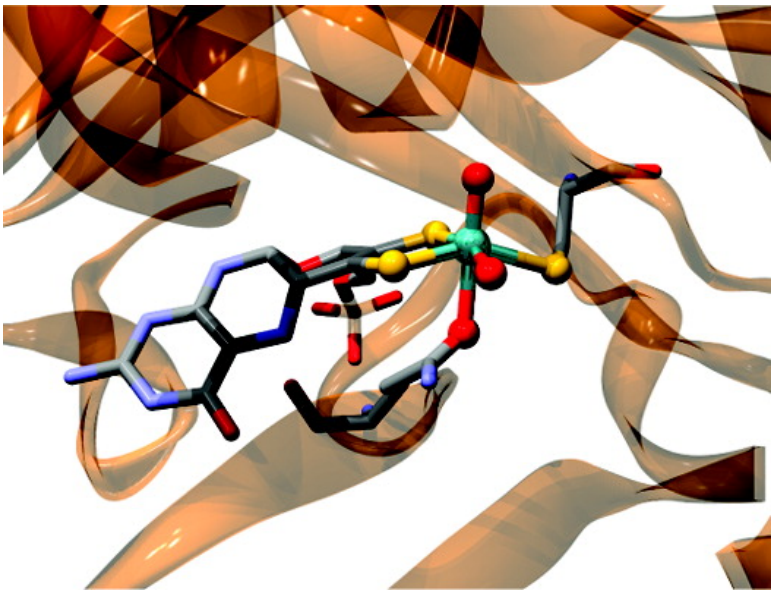

J|A|C|S
ARTICLES
Published on Web 07/04/2007

Modified Active Site Coordination in a Clinical Mutant of Sulfite Oxidase

Christian J. Doonan,[†] Heather L. Wilson,[‡] K. V. Rajagopalan,[‡] Robert M. Garrett,[‡] Brian Bennett,[§] Roger C. Prince,[||] and Graham N. George*,[†]

Contribution from the Department of Geological Sciences, University of Saskatchewan, Saskatoon, Saskatchewan S7N 5E2, Canada, the Department of Biochemistry, School of Medicine, Duke University, Durham, North Carolina 27710, the Department of Biophysics, Medical College of Wisconsin, 8701 Watertown Plank Road, Milwaukee, Wisconsin 53226, and the ExxonMobil Biomedical Sciences, Inc., Annandale, New Jersey 08801

Received February 27, 2007; E-mail: g.george@usask.ca

Abstract: The molybdenum site of the Arginine 160 → Glutamine clinical mutant of the physiologically vital enzyme sulfite oxidase has been investigated by a combination of X-ray absorption spectroscopy and density functional theory calculations. We conclude that the mutant enzyme has a six-coordinate pseudo-octahedral active site with coordination of Glutamine O_ϵ to molybdenum. This contrasts with the wild-type enzyme which is five-coordinate with approximately square-based pyramidal geometry. This difference in the structure of the molybdenum site explains many of the properties of the mutant enzyme which have previously been reported.

Introduction

Sulfite oxidase (SO) is an oxo-transferase enzyme responsible for the physiologically vital oxidation of sulfite to sulfate.[1] Residing in the mitochondrial inner-membrane space, the enzyme is dimeric with a subunit mass of about 52 000. Each monomer contains molybdenum associated with a single pterin cofactor (Moco) and a cytochrome b_5 type heme. The two-electron oxidation of sulfite to sulfate is known to occur at the molybdenum site, which is reduced from Mo^{VI} to Mo^{IV} in the process. The catalytic cycle is completed with reoxidation of the molybdenum first to Mo^{V}, and then to Mo^{VI}, by intramolecular electron transfer to the cytochrome b_5 site, with cytochrome *c* serving as the external electron acceptor.[2,3]

$$\text{Enzyme-Mo}^{VI} + SO_3^{2-} + H_2O \rightarrow \text{Enzyme-Mo}^{IV} + SO_4^{2-} + 2H^+$$

With the exception of nitrogenase,[4] all molybdenum enzymes that have been described to date contain a novel pyranopterin−dithiolene cofactor (known as molybdopterin) in which the Mo atom is coordinated by the dithiolene moiety (Figure 1a).[5,6] In sulfite oxidase, the molybdenum atom is coordinated by two sulfur donors from one dithiolene, two terminal oxygen atoms, and one additional sulfur donor from a cysteine (Cys^{185} in chicken SO or Cys^{207} in human SO).[7] As one of the most intensively studied molybdoenzymes, SO can be regarded as

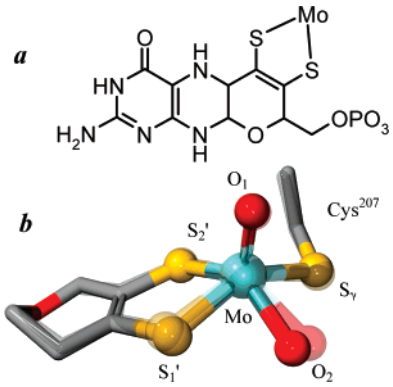

Figure 1. (a) Schematic structure for the molybdopterin molybdenum cofactor. (b) Crystal structure of the active site of photoreduced (probably Mo^{IV}) wild-type and R138Q chicken sulfite oxidases. Only the pyranodithiolene parts of the molybdopterin moiety are shown for clarity. The structure determined for wild-type SO is shown as opaque, while the R138Q structure is shown as a partly transparent model.

[†] University of Saskatchewan.
[‡] Duke University.
[§] Medical College of Wisconsin.
[||] ExxonMobil Biomedical Sciences Inc.

(1) McLeod, R. M.; Farkas, W.; Fridovitch, I.; Handler, P. *J. Biol. Chem.* **1961**, *236*, 1841−1852.
(2) Cohen, H. L.; Betcher-Lange, S.; Kessler, D. L.; Rajagopalan, K. V. *J. Biol. Chem.* **1972**, *247*, 7759−7766.
(3) Johnson, J. L.; Rajagopalan, K. V. *J. Biol. Chem.* **1977**, *252*, 2017−2025.
(4) Rees, D. C.; Tezcan, A.; Haynes, C. A.; Walton, M. Y.; Andrade, S.; Einsle, O.; Howard, J. B. *Philos. Trans. R. Soc. London, Ser. A* **2005**, *363*, 971−984.
(5) Elliot, S. J.; McElhaney, A. E.; Feng, C.; Enemark, J. H.; Armstrong, F. *J. Am. Chem. Soc.* **2002**, *124*, 11612−11613.
(6) (a) Rajagopalan, K. V. *Adv. Enzymol. Relat. Areas Mol. Biol.* **1991**, *64*, 215−290. (b) Rajagopalan, K. V.; Johnson, J. L. *J. Biol. Chem.* **1992**, *267*, 10199−10202.
(7) Kisker, C.; Schindelin, H.; Pacheco, A.; Wehbi, W. A.; Garrett, R. M.; Rajagopalan, K. V.; Enemark, J. E.; Rees, D. C. *Cell* **1997**, *91*, 973−983.
(8) Garrett, R. M.; Johnson, J. L.; Graf, T. N.; Feigenbaum, A.; Rajagopalan, K. V. *Proc. Natl. Acad. Sci. U.S.A.* **1998**, *95*, 6394−6398.
(9) (a) Johnson, J. L.; Coyne, K. E.; Garrett, R. M.; Zabot, M.-T.; Dorche, C.; Kisker, C.; Rajagopalan, K. V. *Hum. Mutat.* **2002**, *20*, 74. (b) Lam, C. W.; Li, C. K.; Lai, C. K.; Tong, S. F.; Chang, K. Y.; Ng, G. S. F.; Yuen, Y. P; Cheng, A. W. F.; Chan, Y. *Mol. Genet. Metab.* **2002**, *75*, 91−95.

the prototypical member of a family of proteins possessing dioxo molybdenum sites in the fully oxidized Mo^{VI} form.[10]

A number of mutations of human SO are known that have very serious pathological consequences, including one recently implicated in a Nevada Leukemia cluster.[11,12] $Arg^{160} \rightarrow Gln$ (R160Q) is a lethal mutation that has been identified in a number of children.[8,9] In this mutant the positively charged arginine residue that is located close to the Moco site is replaced by a neutral glutamine. This mutant SO and the equivalent chicken R138Q mutant have been extensively studied by a number of techniques including enzyme kinetics,[7] protein crystallography,[13] and laser flash photolysis.[14] The mutant has altered steady-state kinetic parameters[7] and shows remarkably decreased rates of intramolecular electron transfer.[14] The greatly increased K_m for sulfite displayed by the mutant has led to the proposal that Arg^{160} functions to attract sulfite to the active site.

All crystal structures of SO that have been reported to date have photoreduced Mo sites (probably Mo^{IV}) due to the large X-ray dose required for crystallographic data acquisition.[15] Protein crystallography of wild-type chicken SO shows a five-coordinate molybdenum site, with an arginine-rich substrate binding pocket ~5 Å from molybdenum. Arg^{138} forms a part of this binding pocket and is the closest of these amino acids to Mo, in conformity with its proposed role. Protein crystallography of R138Q chicken SO reveals modification of the 5 Å pocket with both R138 and R450 affected, with the latter being displaced from its wild-type position. The structure of the molybdenum site, which once again is photoreduced, is five-coordinate[13] and very similar to that of wild-type enzyme.[7] Figure 1b compares the protein crystal structures for the molybdenum site of R138Q and wild-type chicken SO[7,14] with the atoms superimposed to illustrate the local similarity; all atoms can be superimposed to better than 0.5 Å, which is close to the positional error expected for small atoms close to a large atom (i.e., molybdenum) at the resolution of the crystal structures.[7,14] Thus, despite modified properties, a clear role for the Mo site in the molecular basis for the incompetence of this clinical mutant remains unclear. We present herein a high-resolution X-ray absorption spectroscopic study of the oxidized and reduced Mo^{VI} R160Q active site of human SO and show active site structural differences between wild-type and mutant in both oxidized and reduced forms.

Materials and Methods

Sample Preparation. R160Q sulfite oxidase was prepared as described by Garrett et al.[8] All reagents were obtained from Sigma-Aldrich and were of the highest quality available. Samples were prepared in 25 mM MOPS buffer pH 7.0, unless otherwise stated. Reduced enzyme for XAS measurements (approximately 1 mM Mo) was generated by treatment with 10 mM sodium dithionite solution containing a trace (~4 μM) of methyl viologen for approximately 30 s. Samples for XAS were transferred to ($2 \times 10 \times 10$ mm^3) lucite sample cuvettes, rapidly frozen in cold isopentane at −140 °C, and then transferred to liquid nitrogen prior to X-ray absorption spectroscopic data collection. Samples for EPR spectroscopy were approximately 0.1 mM Mo in a mixed buffer system of 0.1 M MES + 0.1 M Bis Tris Propane from which chloride was excluded, and the Mo^{V} oxidation state was generated either by redox titration or by addition of 1 mM (an excess) sulfite.

XAS Data Collection. XAS measurements were conducted at the Stanford Synchrotron Radiation Laboratory (SSRL) with the SPEAR storage ring containing between 80 and 100 mA at 3.0 GeV. Molybdenum K-edge data were collected on the structural molecular biology XAS beamline 9-3 operating with a wiggler field of 2 T. A Si(220) double-crystal monochromator was used. Beamline 9-3 is equipped with a rhodium-coated vertical collimating mirror upstream of the monochromator and a downstream bent-cylindrical focusing mirror (also rhodium-coated). Harmonic rejection was accomplished by setting the cutoff angle of the mirrors to 23 keV. Incident and transmitted X-ray intensities were monitored using argon- or nitrogen-filled ionization chambers. X-ray absorption was measured as the Mo Kα fluorescence excitation spectrum using a 30 element germanium array detector.[16] During data collection, samples were maintained at a temperature of approximately 10 K using an Oxford instruments liquid helium flow cryostat. For each sample, five scans were accumulated, and the energy was calibrated by reference to the absorption of a molybdenum foil measured simultaneously with each scan, assuming a lowest energy inflection point of 20 003.9 eV. The energy threshold of the extended X-ray absorption fine structure (EXAFS) oscillations was assumed to be 20 025.0 eV.

XAS Data Analysis. The EXAFS oscillations $\chi(k)$ were quantitatively analyzed by curve-fitting using the EXAFSPAK suite of computer programs[17] as previously described[18,19] using *ab initio* theoretical phase and amplitude functions calculated using the program FEFF version 8.25.[20,21] No smoothing, filtering, or related operations were performed on the data.

EPR Spectroscopy. Electron paramagnetic resonance (EPR) spectroscopy and data reduction were performed as described by George et al.[22] Spectra were collected using a Varian E109, JEOL RE1X, or Bruker Elexsys instrument. Redox titrations followed the method of Dutton[23] using 40 μM *N*-methylphenazonium methosulfate, *N*-ethylphenazonium ethosulfate, 2-hydroxy-1,4-naphthoquinone, 2-hydroxy-1,4-anthraquinone, indigo disulfonate, indigo trisulfonate, and benzyl viologen as redox mediators between the protein and the platinum measuring electrode. Potentials were measured with respect to a saturated calomel electrode but are reported with respect to the hydrogen electrode by assuming that the calomel electrode has a potential of +247 mV.[24] We used 50 mM bis-tris propane buffers, except for samples at pH 6 for which 50 mM MES was used. Anions such as chloride and sulfate were excluded from the buffers (NaOH or acetic acid were used to adjust pH).

(10) Hille, R. *Chem. Rev.* **1996**, *96*, 2757−2816.
(11) Steinberg, K. K.; Relling, M. V.; Gallagher, M. L.; Greene, C. N.; Rubin, C. S.; French, D.; Holmes, A. K.; Carroll, W. L.; Koontz, D. A.; Sampson, E. J.; Satten, G. A. *Environ. Health Perspect.* **2007**, *115*, 158−164.
(12) This mutation is G628A which is in the untranslated 5′-region of the sulfite oxidase gene, which may somehow lead to decreased expression of sulfite oxidase. The occurrence of leukemia is also linked to the environmental presence of tungsten,[11] and we can conjecture that the mutation decreases gene expression, which combined with molybdenum antagonism by tungsten significantly lowers sulfite oxidase levels. Further work is clearly needed to establish the mechanism.
(13) Karakas, E.; Wilson, H. L.; Graf, T. N.; Xiang, S.; Jaramillo-Busquets, S.; Rajagopalan, K. V.; Kisker, C. *J. Biol. Chem.* **2005**, *280*, 33506−33515.
(14) Feng, C.; Wilson, H. J.; Hurley, J. K.; Hazzard, J. T.; Tollin, G.; Rajagopalan, K. V.; Enemark, J. H. *Biochemistry* **2003**, *42*, 12235−12242.
(15) George, G. N.; Pickering, I. J.; Kisker, C. *Inorg. Chem.* **1999**, *38*, 2539−2540.
(16) Cramer, S. P.; Tench, O.; Yocum, M.; George, G. N. *Nucl. Instrum. Methods* **1988**, *A266*, 586−591.
(17) http://ssrl.slac.stanford.edu/exafspak.html.
(18) George, G. N.; Garrett, R. M.; Prince, R. C.; Rajagopalan, K. V. *J. Am. Chem. Soc.* **1996**, *118*, 8588−8592.
(19) Doonan, C. J.; Stockert, A.; Hille, R.; George, G. N. *J. Am. Chem. Soc.* **2005**, *127*, 4518−4522.
(20) Rehr, J. J.; Mustre de Leon, J.; Zabinsky, S. I.; Albers, R. C. *J. Am. Chem. Soc.* **1991**, *113*, 5135−5140.
(21) Mustre de Leon, J.; Rehr, J. J.; Zabinsky, S. I.; Albers, R. C. *Phys. Rev. B* **1991**, *44*, 4146−4156.
(22) George, G. N.; Prince, R. C.; Kipke, C. A.; Sunde., R. A.; Enemark, J. E. *Biochem. J.* **1988**, *256*, 307−309.
(23) Dutton, P. L. *Methods Enzymol.* **1978**, *24*, 431−446.
(24) Clark, W. M. *Oxidation-Reduction Potentials of Organic Systems*; Williams and Wilkins: Baltimore, MD, 1960.

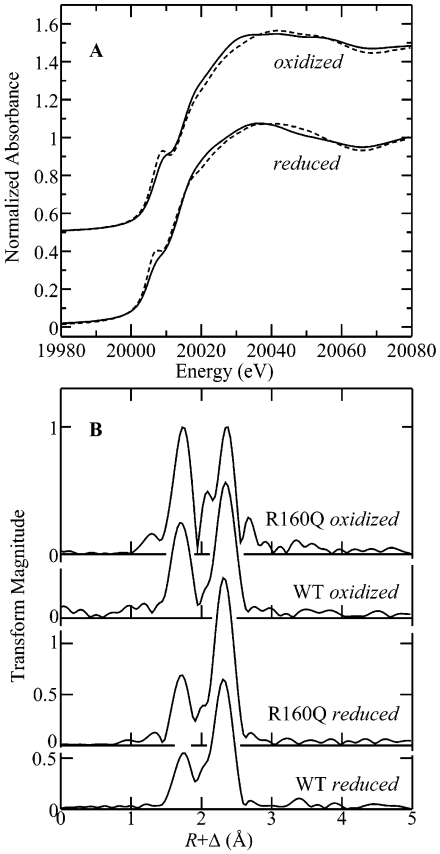

Figure 2. (A) Comparison of the molybdenum K near-edge spectra R160Q human sulfite oxidase (solid lines) with those of wild-type enzyme (broken lines), in oxidized (*a*) and reduced (*b*) forms. (B) Comparison of Mo K-edge EXAFS Fourier transforms of wild-type and R160Q human sulfite oxidase in both oxidized and reduced forms. Transforms are phase corrected for Mo−S backscattering and are restricted to the same *k*-range (1−18 Å^{-1}).

Molecular Modeling. Density Functional Theory (DFT) molecular modeling used the program Dmol3 Materials Studio Version 3.2.[25,26] We expect bond-length accuracies of around 0.05 Å and good estimates of energetic trends between postulated molecular entities. The Becke exchange[27] and Perdew correlation[28] functionals were used to calculate both the potential during the self-consistent field procedure and the energy. Double numerical basis sets included polarization functions for all atoms. Calculations were spin-unrestricted, and all electron relativistic core potentials were used. No symmetry constraints were applied, and optimized geometries used energy tolerances of 2.0 × 10^{-5} hartree.

Results and Discussion

Mo K Near-Edge X-ray Absorption Spectra. Figure 2A compares the molybdenum K near-edge spectrum of oxidized and reduced R160Q SO with corresponding spectra for samples of wild-type enzyme. Near-edge spectra are comprised of transitions of the core−electron (i.e., Mo 1s) to bound states involving the frontier molecular orbitals of the system and are thus sensitive to electronic structure and hence to geometry. The lowest energy peak at ca. 20 009 eV is observed in both spectra and is attributed to a Mo 1s → Mo═O π* transition.[29] The contrasting spectra of wild-type and R160Q SO shown in Figure 2 clearly indicate structural differences between wild-type and mutant active sites.

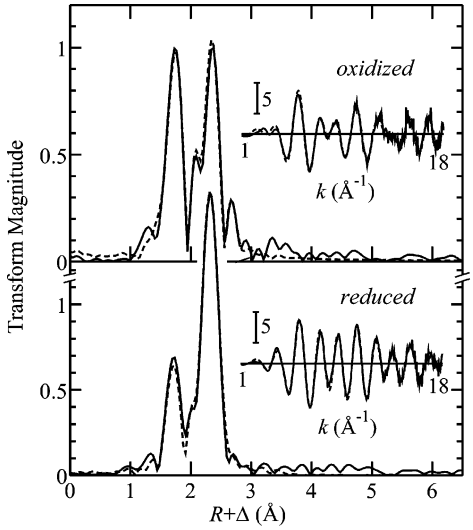

Figure 3. Mo K-edge EXAFS Fourier Transforms (Mo−S phase-corrected), plus the EXAFS spectra (shown in insets), for oxidized and reduced R160Q sulfite oxidase. Solid lines show the experimental data, and broken lines show the best fits using the parameters given in Table 1.

Molybdenum K-Edge EXAFS. Figure 2B compares the EXAFS Fourier transforms of wild-type and R160Q SO. The differences between the mutant and wild-type transforms clearly show that the mutant has modified Mo coordination in both oxidized and reduced forms. Figure 3 shows the extended X-ray absorption fine structure (EXAFS) Fourier transform of R160Q SO in oxidized and reduced forms, together with the results of the curve-fitting analysis. As we have discussed above, the only available quantitative structural information on oxidized sulfite oxidase is from EXAFS spectroscopy. For oxidized wild-type SO only two different EXAFS contributions are resolved, even with data extending to 25 Å^{-1}.[30] The data are described by two Mo═O at an average distance of 1.72 Å and three Mo−S at 2.42 Å, with individual Mo═O and Mo−S bond lengths differing by less than 0.05 Å.[30] In contrast, the EXAFS of oxidized R160Q enzyme requires a total of four different EXAFS interactions to fit the data, and this is illustrated in Figure 4. Curve-fitting analysis shows two Mo═O at 1.73 Å, one Mo−O at 2.22 Å, two Mo−S at 2.44 Å, and a long Mo−S at 2.58 Å (Table 1), which indicates a total of six ligands to Mo.[31] For molybdenum, a likely geometry for such a six-coordinate species is pseudo-octahedral, and in this case two ligands will be positioned *trans* to each of the two oxo ligands and significant *trans*-effect elongation of these bonds is expected. The long Mo−S bond detected by EXAFS is thus likely to originate from sulfur coordination *trans* to one of the two Mo═O groups. Examination of the Cambridge Structural database[33] searching for dioxo Mo^{VI} species with a Mo−S positioned *trans* to a Mo═O indicates a *trans*-effect Mo−S

(25) Delley, B. *J. Chem. Phys.* **1990**, *92*, 508−517.
(26) Delley, B. *J. Chem. Phys.* **2000**, *113*, 7756−7764.
(27) Becke, A. D. *J. Chem. Phys.* **1988**, *88*, 2547−2553.
(28) Perdew, J. P.; Wang, Y. *Phys. Rev. B* **1992**, *45*, 13244−13249.
(29) Kutzler, F. W.; Natoli, C. R.; Misemer, D. K.; Donaich, S.; Hodgson. K. O. *J. Chem. Phys.* **1980**, *73*, 3274−3288.
(30) Harris, H. H.; George, G. N.; Rajagopalan, K. V. *Inorg. Chem.* **2006**, *45*, 493−495.
(31) Normally, distinguishing between five-coordinate (e.g., oxidized wild-type SO) and six-coordinate (e.g., oxidized R160Q SO) sites would be challenging for EXAFS. The resolution of four discrete interactions (Figure 4) means that in this case it is straightforward to determine that oxidized R160Q SO is six-coordinate.
(32) George, G. N.; Hilton, J.; Temple, C.; Prince, R. C.; Rajagopalan, K. V. *J. Am. Chem. Soc.* **1999**, *121*, 1256−1266.
(33) Allen, F. H.; Kennard, O.; Watson, D. G. *Struct. Correl.* **1994**, *1*, 71−110.

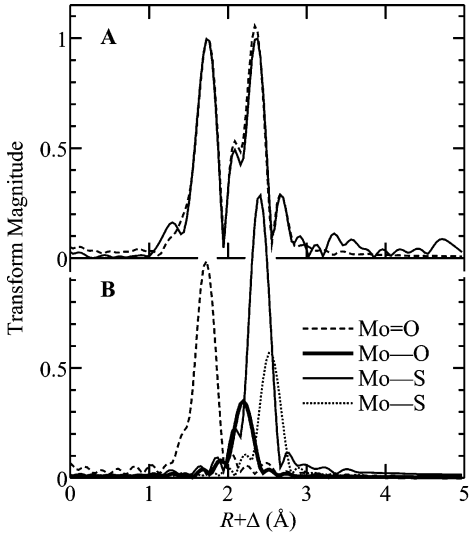

Figure 4. (A) Mo K-edge EXAFS Fourier transform (Mo—S phase-corrected) of oxidized R160Q sulfite oxidase. The solid line shows experimental data, and the broken line the best fit. (B) Breakdown of the fit, with the Fourier transform of the four individual EXAFS contributions shown in different line styles.

bond-length range of 2.53 to 2.78 Å. By comparison the mean Mo—S bond length for dioxo Mo^{VI} species with sulfur coordinated *cis* to both Mo═O groups is 2.42 Å.[33] The observed bond length for *trans* ligands depends approximately on the O═Mo—S bond angle, with the most nearly linear (~166°) having the longest, and the most acute (~144°) having the shortest Mo—S bond length. The 2.58 Å Mo—S bond length determined by EXAFS is thus within the range of Mo═O *trans*-effect elongated sulfur ligands and is notably absent in wild-type SO.[30] The correlation observed in the data from the Cambridge Structural database[34] suggests an O═Mo—S bond angle in the range 145° to 154°. The EXAFS also shows two Mo—S bonds at bond lengths of 2.44 Å, with no Mo═O *trans*-elongation. Thus, our EXAFS data suggest a six-coordinate site arising from coordination of an additional Mo—O ligand. These findings are consistent with the marked difference observed in the UV—visible absorption spectra between the isolated Mo domains[35] of wild type SO and the R160Q mutant,[8] as an altered active site structure is expected to give rise to a quite distinct electronic spectrum.

The EXAFS analysis of the data from reduced R160Q SO indicates a single Mo═O at 1.71 Å, plus three equivalent (within the resolution of our measurements ~0.086 Å) Mo—S at 2.41 Å, and either one or two Mo—O. A single Mo—O gives a bond length of 2.22 Å, while two different Mo—O give bond lengths of 2.21 and 2.32 Å and a slightly better fit (Table 1). Unfortunately, this improvement is marginal, and we cannot unambiguously determine whether one or two Mo—O ligands are present.[36] The results from protein crystallography clearly indicate a five-coordinate site, which favors the first alternative, but the EPR spectroscopy (considered below) indicates the presence of multiple forms of the active site in the reduced enzyme.

Electron Paramagnetic Resonance Spectroscopy. Wild-type SO gives Mo^{V} EPR signals that can be divided into three different categories (Table 2). The high-pH signal occurs at low anion concentrations and at high-pH values, while the low-pH/Cl^- signal occurs at low pH and high chloride.[37,38] A third category of signals are those from oxy-anion complexes, which tend to form at low pH and high oxy-anion concentrations. SO Mo^{V} EPR signals arising from anion complexes have been described for phosphate, arsenate, and sulfite (or sulfate).[22,37,39−42] Analysis of the ^{31}P hyperfine interaction of the phosphate signal and structural analysis of the arsenate signal using EXAFS indicate that in both cases the anion is coordinated to molybdenum via one of its oxygen ligands.[22,39,40]

Figure 5 shows the three primary Mo(V) EPR signals that can be obtained from R160Q SO. The signals are related by pH, with at least two different pK_a values involved. Figure 5A shows a pH titration of R160Q Mo(V) EPR signals. The high-pH signal (Figure 5Aa) is very similar to that observed for wild-type SO, suggesting a nearly identical coordination at high pH, and is in agreement with the reduced sites determined by crystallography. The two low-pH signals are related to each other, and the high-pH signal is by ionizable groups (amino acid side chains) with pK_a values of 8.0 and 6.1, respectively:

$$\text{Low-pH Type 1} \overset{pK_{a_1}=6.1}{\rightleftharpoons} \text{Low-pH Type 2} + H^+ \overset{pK_{a_2}=8.0}{\rightleftharpoons} \text{High pH} + 2H^+$$

The two low-pH signals show no clear structure from proton hyperfine interactions and are essentially identical when developed in deuterated water (not illustrated). Figure 6 compares the Mo^{V} EPR redox titrations of wild-type and R160Q SO. The conditions for wild-type enzyme were chosen so as to produce a single Mo^{V} EPR signal under the two conditions used (the low pH/Cl^- species at low pH and the high pH species at high pH), and the conditions for the R160Q low-pH redox titration were chosen so that both the low-pH type 1 and type 2 signals would be observed. No difference in redox behavior was detected between the type 1 and type 2 low pH signals. At pH 9 the midpoint potentials E_m of wild-type enzyme are −206 mV (Mo^{IV}/Mo^{V}) and +30 mV (Mo^{V}/Mo^{VI}), and these are shifted to lower values in R160Q SO, −247 and −27 mV for $E_m(Mo^{IV}/Mo^{V})$ and $E_m(Mo^{V}/Mo^{VI})$, respectively. The E_m values are shifted to higher values at lower pH (wild-type pH 6.0, 0.1 M Cl, R160Q pH 6.5): $E_m(Mo^{IV}/Mo^{V}) = -62$ mV and $E_m(Mo^{V}/Mo^{VI}) = +150$ mV, for wild-type; −127 mV and +122 mV for R160Q SO, respectively. This is close to the theoretically

(34) An approximately linear relationship between the Mo—S bond length and O═Mo—S bond angle is observed (correlation coefficient 0.955).
(35) Features attributable to molybdenum cannot readily be observed in the UV—visible spectrum of intact sulfite oxidase because of the relatively very intense absorption of the cytochrome moiety.
(36) We note that previous high-resolution EXAFS spectroscopy[30] means that there is substantially less ambiguity in the number of Mo—O ligands present in wild-type enzyme. In this work EXAFS which extended to $k = 25$ Å^{-1} was used to resolve the Mo—O interaction from the overlapping Mo—S interaction.

(37) Lamy, M. T.; Gutteridge, S.; Bray, R. C. *Biochem. J.* **1980**, *185*, 397−403.
(38) Bray, R. C.; Gutteridge, S.; Lamy, M. T.; Wilkinson, T. *Biochem. J.* **1983**, *211*, 227−236.
(39) Pacheco, A.; Basu, P.; Borbat, P.; Raitsimring, A. M.; Enemark, J. H. *Inorg. Chem.* **1996**, *35*, 7001−7008.
(40) George, G. N.; Garrett, R. M.; Graf, T.; Prince, R. C.; Rajagopalan, K. V. *J. Am. Chem. Soc.* **1998**, *120*, 4522−4523.
(41) Bray, R. C.; Lamy, M. T.; Gutteridge, S.; Wilkinson, T. *Biochem. J.* **1982**, *201*, 241−243.
(42) We note that the Mo^{V} EPR signal attributed to a coordination of sulfite by Bray et al.[41] has alternatively been attributed to a sulfate coordinated species [Astashkin, A. V.; Hood, B. L.; Feng, C.; Hille, R.; Mendel, R. R.; Raitsimring, A. M.; Enemark, J. H. *Biochemistry* **2005**, *44*, 13274−13281].

Table 1. EXAFS Curve-Fitting Parameters[a]

	Mo–S			Mo–O				
sample	*N*	*R*	σ^2	*N*	*R*	σ^2	ΔE_0	*F*
R160Q, oxidized	2	2.442(3)	0.0021(1)	2	1.725(2)	0.0023(1)	−10.7(6)	0.261
	1	2.580(4)	0.0023(2)[b]	1	2.217(5)	0.0025(9)		
R160Q, reduced pH 7	3	2.413(1)	0.0027(1)	1	1.706(1)	0.0015(1)	−10.3(3)	0.168
				1	2.221(4)	0.0020(2)		
	3	2.409(2)	0.0029(1)	1	1.707(1)	0.0015(1)	−9.1(5)	0.165
				1	2.215(6)	0.0028(8)		
				1	2.32(1)	0.0031(8)		

[a] Coordination numbers, *N*, interatomic distances, *R* (Å), Debye−Waller factors, σ^2 (Å^2), and threshold energy shifts, ΔE_0 (eV). Values in parentheses are the estimated standard deviations (precisions) obtained from the diagonal elements of the covariance matrix. The accuracies will be much greater than these values and are generally accepted to be ±0.02 Å for bond lengths and ±20% for coordination numbers and Debye−Waller factors. The fit-error function *F* is defined as $F = \sqrt{\Sigma k^6(\chi_{calcd}-\chi_{expt})^2/\Sigma\chi^2_{expt}}$, where the summations are over all data points included in the refinement. [b] The value for this Debye−Waller factor is smaller than might be expected for such a long Mo−S interaction; however we note that similar Debye−Waller factors (i.e., ∼0.0026 Å^2) have been observed for compounds showing pronounced Mo=O induced *trans*-elongation of Mo−S bond lengths.[32]

Table 2. Mo^V EPR Spin Hamiltonian Parameters[a]

sample	parameter	*x*	*y*	*z*
R160Q high pH	**g**	1.9526	1.9636	1.9875
	Δ	0.38	0.39	0.30
	A(^{1}H)[b]	−10	−10	20
R160Q low pH 1	**g**	1.9514	1.9708	2.0061
	Δ	0.22	0.27	0.32
R160Q low pH 2	**g**	1.9391	1.9604	1.9978
	Δ	0.27	0.24	0.30

[a] *g*-Values, line widths (mT), and hyperfine (MHz) obtained from the computer simulations shown in Figure 5. [b] Note that these are approximate values obtained by computer simulation using non-colinear **g** and **A** at the trimagic angle.[49]

expected −59 mV per pH unit change if the reactions involve a single proton per electron, although we note that the different molybdenum coordination environments of the different signal-giving species will complicate the relationship. Compared to wild-type SO, R160Q is thus effectively harder to reduce, and the reduced mutant enzyme will itself be a better reducing agent.

The transition between wild-type SO low-pH and high-pH signals depends on an ionizable group with a pK_a of less than 6.8 in the absence of high concentrations of exogenous anions. It seems probable that the ionizable group detected by Mo^V EPR in wild-type SO is one of the two ionizable groups that influence the EPR spectra of R160Q SO. These are likely to be amino acid side chains in proximity to the Moco site. One candidate is Tyr,[343] which has been implicated as being important in catalytic turnover of the enzyme[43] and in electron transfer between the cytochrome b_5 moiety and the Moco.[44] Furthermore, the bacterial sulfite dehydrogense of *Starkeya novella*[45,46] (previously *Thiobacillus novella*) only shows high-pH Mo^V EPR signals;[45,47] however when Tyr[236] (the analogous amino acid to SO Tyr[343]) is modified to a phenylalanine, characteristic low-pH Mo^V EPR signals very similar to those observed for WT SO can be developed by lowering the pH.[48] Free tyrosine in aqueous solution has a side-chain pK_a of 10.1, but this will be

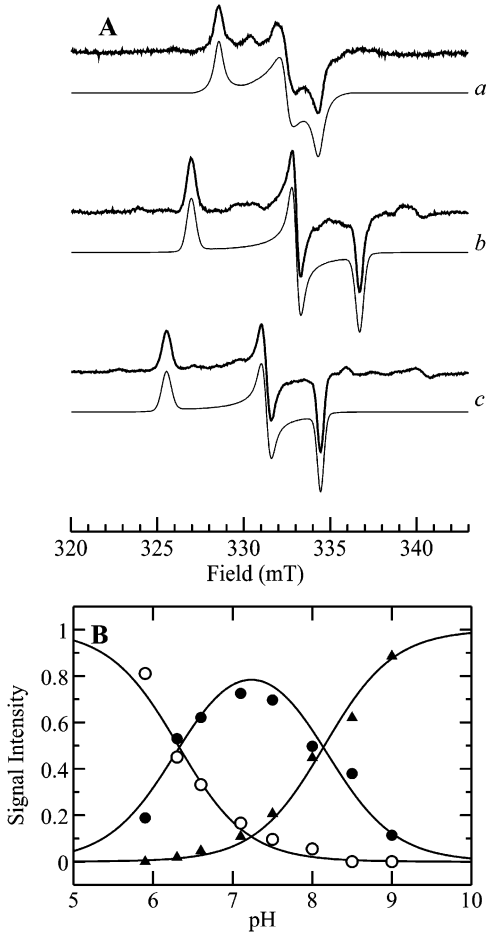

Figure 5. Mo^V EPR spectra of R160Q sulfite oxidase. (A) The three different types of EPR spectra detected for R160Q SO aligned to a microwave frequency of 9.1367 GHz. Experimental spectra are shown as bold lines, while simulations computed using the parameters given in Table 2 are shown as fine lines. *a* shows the high-pH spectrum, *b* shows the low-pH type 2, and *c* shows the low-pH type 1 spectrum. (B) pH dependence of the Mo^V EPR signals. The points show the experimental Mo^V integrated EPR signal intensity: ● low-pH type 1, ▲ low-pH type 2, and ○ high pH. The lines are computed curves for the equilibrium discussed in the text, using pK_a values of 6.1 and 8.0.

significantly shifted (to a lower value) by the presence of the highly basic residues in the active site of SO, so that one of the two observed pK_a values of R160Q SO could be that of Tyr.[343] The two low-pH species are quite similar EPR signals (different

(43) Wilson, H. L.; Rajagopalan, K. V. *J. Biol. Chem.* **2004**, *279*, 15105−15113.
(44) Feng, C.; Wilson, H. L.; Hurley, J. K.; Hazzard, J. T.; Tollin, G.; Rajagopalan, K. V.; Enemark, J. H. *J. Biol. Chem.* **2003**, *278*, 2913−2920.
(45) Kappler, U.; Bennett, B.; Rethmeier, J.; Schwarz, G.; Deutzmann, R.; McEwan, A. G.; Dahl, C. *J. Biol. Chem.* **2000**, *275*, 13202−13212.
(46) Kappler, U.; Bailey, S. *J. Biol. Chem.* **2005**, *280*, 24999−25007.
(47) Doonan, C. J.; Kappler, U.; George, G. N. *Inorg. Chem.* **2006**, *45*, 7488−7492.
(48) Kappler, U.; Bailey, S.; Feng, C.; Honeychurch, M. J.; Hanson, G. R.; Bernhardt, P. V.; Tollin, G.; Enemark, J. H. *Biochemistry* **2006**, *45*, 9696−9705.

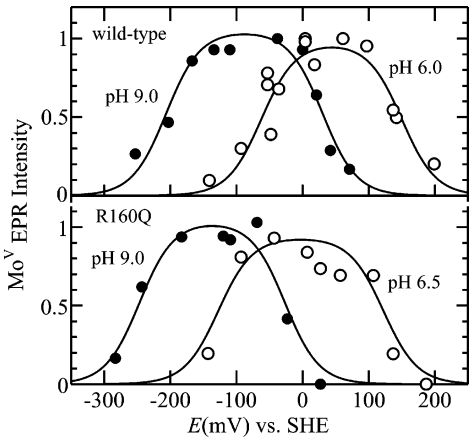

Figure 6. Mo^V redox titrations of wild-type and R160Q sulfite oxidase, under conditions for high-pH ● and low-pH ○ Mo^V EPR signals. For wild-type enzyme the low-pH enzyme had 0.1 M NaCl added in order to ensure 100% of the low-pH species.

g-values, but similar *g*-anisotropies, a similar lack of resolved proton hyperfine splitting, and indistinguishable redox potentials), and it seems likely that the two low-pH species are structurally similar. Thus ionization of nearby Tyr^{343} might induce a subtle comformational change in the active site, which is reflected in the two different R160Q low-pH Mo^V EPR signals. A candidate for the second residue that influences the Mo^V EPR spectra might be the Gln^{160} residue, and we will return to considering this residue later.

The lack of resolved proton splitting in the two low-pH signals is important and has bearing on the structure of the signal giving species. The high-pH signal of wild-type SO has no resolved hyperfine splitting but nevertheless possesses a strongly coupled proton. This has been detected by the observation of formally forbidden $\Delta m_I = \pm 1$ transitions[49] and by pulsed EPR spectroscopy.[50] George postulated that the proton hyperfine tensor from the hydrogen in an Mo−OH group is oriented close to the trimagic angle[49] where the dipole coupling along each direction of g_x, g_y, and g_z will be zero, while later work using pulsed EPR spectroscopy[50] concluded that the proton splitting was hidden by rotation of the Mo−OH group about the Mo−O bond to yield a static distribution of Mo−O−H orientations and a corresponding ensemble of hyperfine interactions.[50,51] At present neither of these two alternatives has been definitively proven. Anion-bound species such as the phosphate, sulfite (or sulfate), and arsenite compexes also show no hyperfine splitting from an exchangeable proton[22,37,39−42] because in these cases the Mo−OH group is lacking. No splitting from coupled exchangeable protons is detected in any R160Q EPR signal at X-band microwave frequencies. The lack of resolved proton hyperfine splittings in the R160Q low-pH signals suggests that either their protons are oriented in an unfavorable geometry (we will consider this further below) or alternatively the Mo−OH group has been displaced by coordinaton of sulfite which was used as a reductant to develop the Mo^V EPR signals or from sulfate (the product of the reduction). Although we cannot

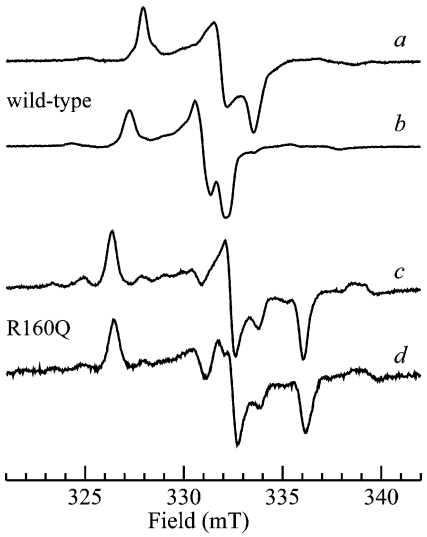

Figure 7. Effects of addition of phosphate on Mo^V EPR signals of wild-type and R160Q sulfite (pH 8), showing the wild-type enzyme in the absence (*a*) and presence (*b*) of 60 mM sodium phosphate and R160Q enzyme in the absence (*c*) and presence (*d*) of 60 mM sodium phosphate.

exclude it,[52] we consider sulfur anion coordination the less likely of the two possibilities as identical Mo^V EPR signals were observed in redox titrations containing only traces of sulfite, and experiments using a large excess (20 mM) of sulfite did not perturb the apparent pK_a (pK_{a_2}) between R160Q high-pH and the R160Q low-pH type 2 signals (not illustrated).

In marked contrast to wild-type SO, anions such as phosphate[22,39,53] had no effect on the Mo^V EPR of R160Q sulfite oxidase. Figure 7 shows this for addition of 60 mM phosphate to wild-type and R160Q SO. The characteristic Mo^V EPR signal of the phosphate complex[22,53] is formed with the wild-type enzyme, whereas the effects of phosphate on R160Q are only very slight and not resolvable as any discrete Mo^V signal under the conditions of our experiments. This is consistent with the proposed role of Arg^{160} in stabilizing anion complexes.

Molecular Modeling and the Structure of the Mutant Molybdenum Site. The six-coordinate active site of the oxidized enzyme is of considerable interest. The obvious candidates for the additional ligand to molybdenum are O_ϵ and N_ϵ of Gln.[160] Amides can potentially coordinate metal ions in three different ways: first through the $-NH_2$ group of the amide, second via a coordinate bond through the carbonyl of the amide, and third via formation of the resonance form imidic acid [−(HN═)C−OH] and binding metal through the oxygen.

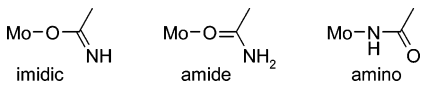

We note in passing that the first of these two forms is related by protonation of the amide group, which provides another possible candidate for the origin of the pH induced changes

(49) George, G. N. *J. Magn. Reson.* **1985**, *64*, 384−394.
(50) Astashkin, A. V.; Mader, M. L.; Pacheco, A.; Enemark, J. H.; Raitsimring, A. M. *J. Am. Chem. Soc.* **2000**, *122*, 5294−5302.
(51) Enemark, J. H.; Astashkin, A. V.; Raitsimring A. M. *J. Chem. Soc., Dalton Trans.* **2006**, 3501−3514.
(52) DFT calculations support the possibility of a six-coordinate Mo with coordinated sulfite or sulfate. The geometry is very similar to that discussed below for protonated species, except that the S−OH is hydrogen bonded to the axial Mo═O group (not illustrated).
(53) Gutteridge, S.; Lamy, M. T.; Bray, R. C. *Biochem. J.* **1980**, *191*, 285−288.
(54) Garrett, R. M.; Johnson, J. L.; Graf, T. N.; Feigenbaum, A.; Rajagopalan, K. V. *Proc. Natl. Acad. Sci. U.S.A.* **1998**, *95*, 6394−6398.
(55) Bray, R. C.; Lamy, M. T.; Gutteridge, S.; Wilkinson, T. *Biochem. J.* **1982**, *201*, 241−243.

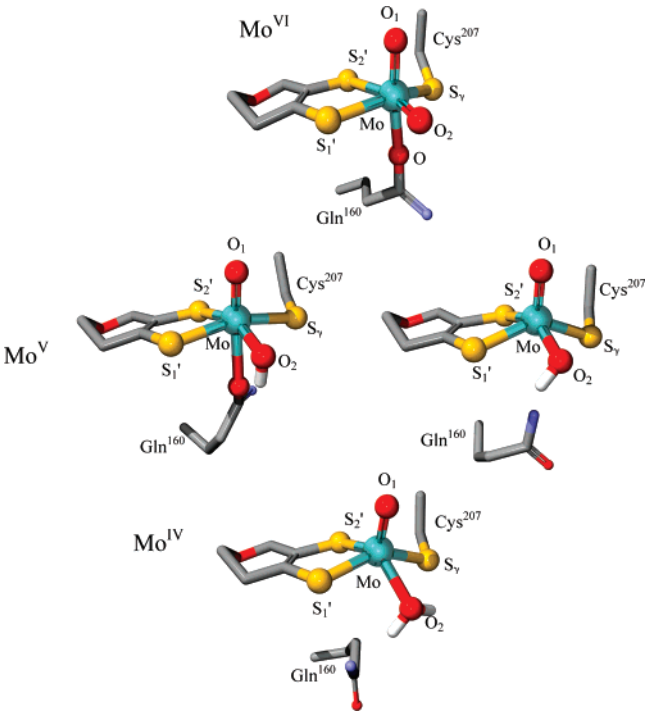

Figure 8. Density functional theory energy-minimized structure for the active site of R160Q SO in the three different oxidation states. All but the Mo−O_2 bound hydrogen atoms have been omitted for clarity.

observed in the Mo^V EPR (i.e., between low-pH types 1 and 2). A search of the Cambridge Structural Database[33] reveals Mo^{VI} *cis*-dioxo examples of all three modes of coordination. For ligands coordinated approximately *trans* to one Mo═O the Cambridge database gives average bond lengths of 2.21, 2.22, and 2.30 Å for bonds formulated as imidic, amide, and amino coordinations, respectively. An alternative explanation of the distant oxygen might be an additional water or −OH ligand to Mo that is somehow stabilized by the presence of Gln.[160] We tested the hypothesis of Gln^{160} coordination using constrained density functional theory (DFT) calculations of the active site structure. DFT calculations have to be limited to a small number of atoms because the processor time required scales approximately as the square of the number of electrons considered in the calculation. We truncated the active site structure at the furan ring of the molybopterin and at the alpha carbons of Cys^{207} and Gln^{160} (Figure 8), but we also constrained the four most distant atoms of the furan ring (i.e., not the ditholene carbons) and the amino acid alpha carbons to their crystallographically determined positions.[13] Molybdenum coordination by a carbonyl was not supported by our calculations, as in all cases tested the carbonyl dissociated. Similarly Mo−OH and Mo−OH_2 were found to be unstable in our calculations. On the other hand, both the nitrogen-coordinated amide and the oxygen-coordinated imide structures readily converged, with very close to the same minimum energy. EXAFS alone cannot distinguish between Mo−O and Mo−N coordination, and we are thus unable to discriminate between oxygen and nitrogen as the ligand. The energy of the nitrogen coordinated species was marginally lower (0.3 eV) than that of the oxygen coordinated species, but the correspondence between the DFT of the oxygen coordinated species and the EXAFS-derived bond lengths is much better for the oxygen-bound complex (although the *trans*-elongated Mo−S_2' bond length is slightly outside the usual 0.05 Å error

Table 3. Selected Interatomic Distances[a] for DFT Computed Structures vs Crystallography

bond	Mo^{VI}	Mo^V	Mo^V	Mo^{IV}	crystallography[b]
Mo−O_1	1.748	1.724	1.721	1.716	1.6
Mo−O_2	1.755	2.007	2.001	2.331	2.2
Mo− S_1'	2.495	2.482	2.419	2.389	2.3
Mo− S_2'	2.683	2.496	2.443	2.382	2.4
Mo−S_γ(C207)	2.521	2.478	2.424	2.426	2.5
Mo−O_ϵ(R160)	2.256	2.375	−	−	−

[a] Interatomic distances are given in Å. [b] Values taken from the coordinates deposited in the protein structure database.[13]

expected for unconstrained DFT). In either case, our calculations clearly demonstrate that Gln^{160} can potentially coordinate Mo in an axial position to form a pseudo-octahedral geometry. When the positional constraints described above were relaxed, the energy minimized structures were very similar (not illustrated), but the positions of the constrained carbons and their neighbors were significantly altered (especially the outer carbons of the amino acids). The DFT calculations also allow us to assign the elongated Mo−S ligand to Mo−S_2' (Figure 8, Table 1).

Several different DFT optimized geometries for the reduced site were tested for both Mo^V and Mo^{IV} oxidation states. Selected interatomic distances obtained from DFT are compared with those from crystallography in Table 3. For Mo^V species, the O_2 atom was formulated as an Mo−OH ligand, while, for Mo^{IV} species, the O_2 atom was formulated as Mo−OH_2. In both oxidation states, amine coordinated complexes were unstable and converged to a structure in which the amine had dissociated by abstracting a proton from the Mo−OH or Mo−OH_2. In the Mo^{IV} oxidation state, Gln^{160} oxygen-coordinated alternatives also dissociated from Mo, yielding a five-coordinate active site with a very similar geometry to that determined by protein crystallography. An interesting difference is that the positions of the $O_\epsilon{}^1$ and $N_\epsilon{}^2$ atoms of Gln^{160} are reversed from those shown in the crystal structure. As oxygen and nitrogen atoms will appear essentially identical to protein crystallography it seems possible that the position revealed by DFT is that found in the enzyme, although refinements with more amino acid residues in the active site would provide additional confidence. With the two Gln^{160} oxygen-coordinated Mo^V structures tested, amide-coordinated species converged to structures in which Gln^{160} did not coordinate the molybdenum, but the imidic-coordinated species converged to coordinated forms, and this suggests the possibility of a six-coordinate active site for this oxidation state. Our Mo^V EPR results suggest that the high-pH signal is quite similar to the analogous signal observed for wild-type enzyme, which is thought to be a five-coordinate species with an equatorial Mo−OH. In contrast, the two different low-pH signals, while somewhat similar to each other, are quite unlike any Mo^V EPR signal obtained from the wild-type enzyme. Thus, we hypothesize that the signal-giving species for the R160Q low-pH signals are six-coordinate structures with Gln^{160} coordinated to Mo through O_ϵ of this residue. We further suggest that the signal-giving species for the R160Q high-pH signal corresponds to the five-coordinate structure in which Gln^{160} is dissociated from Mo. We now turn to the lack of observable hyperfine splitting from an exchangeable proton in the R160Q low-pH signal. A Mo^V active site structure lacking an Mo−OH ligand is very difficult to rationalize, and it seems likely that the absence of proton hyperfine splitting is the result of the proton being in an unfavorable geometry for a large hyperfine splitting

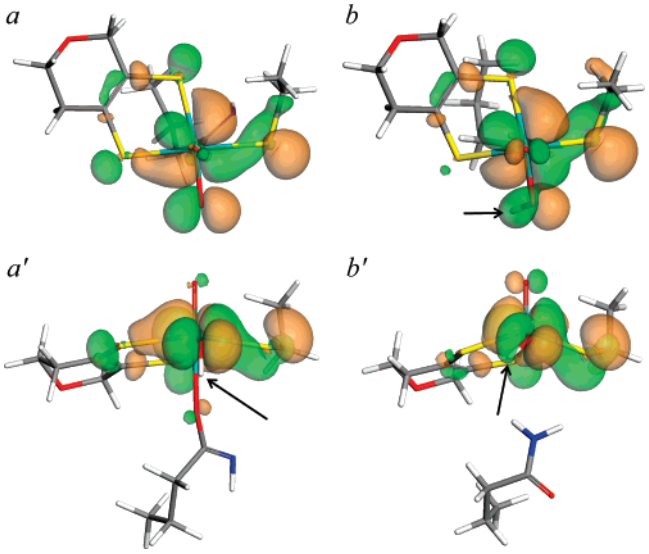

Figure 9. Highest occupied molecular orbitals for energy-minimized Mo^V structures with six-coordinate (*a* and *a′*) and five-coordinate (*b* and *b′*) molybdenum. Panels *a* and *b* show the view from above, looking approximately along the Mo═O_1 bond, while panels *a′* and *b′* show the view looking along the Mo—O_2 bond. The orientation of the Mo—OH proton is shown by the arrows and can be seen to be pointed away from the plane of the orbital in the six-coordinate case (in *a* the proton is hidden beneath the Mo—O_2 bond).

in the signal-giving species. Our DFT energy-minimized structures show Mo—OH proton orientations consistent with this hypothesis (Figure 8). For the six-coordinate species the proton of the Mo—OH is oriented out of the plane of the paramagnetic ground-state molecular orbital (Figure 9), and this would give rise to much smaller hyperfine couplings than if it were oriented in the plane of this orbital. With the five-coordinate species, on the other hand, the proton is oriented close to the plane of the ground-state orbital (Figure 9), which would give rise to larger hyperfine couplings, and (at least in wild-type enzyme) the high-pH signal does possess a strongly coupled proton (although as we have discussed, it does not show a proton splitting at X-band microwave frequencies). Our DFT calculations thus provide a plausible explanation for the Mo^V EPR signals observed for R160Q SO. As we have discussed above, because sulfite was added to the samples to develop the Mo^V oxidation state, the further possibility of a sulfite-coordinated form must also be considered. As noted above, we consider this possibility unlikely but still a possibility. In this case the Mo—OH group would be replaced by coordinated sulfite (Mo—O—S(O)OH), and proton hyperfine is not expected to be observed. DFT energy-minimized structures (not illustrated) converge to six-coordinate species that are similar to those containing Mo—OH groups, showing hydrogen bonding between the ═S—OH proton and the Mo═O group.

Finally, the fundamental differences in coordination between oxidized wild-type SO and R160Q SO suggest a molybdenum-centered molecular basis for aspects of the kinetic incompetence of the mutant. Current postulated catalytic mechanisms for SO all involve coordination of substrate to molybdenum, and a variety of anion complexes have been observed spectroscopically.[22,40] In these complexes oxy-anions coordinate the metal via oxygen to form a Mo—O—A arrangement (where A is the central atom of the oxy-anion).[39,40,53] In R160Q SO such coordination of substrate to the mutant enzyme would require displacement of coordinated Gln^{160} in the oxidized enzyme. Furthermore, the anion-complex stabilizing effects expected from the proximity of a highly basic residue such as Arg^{160} will be missing from the mutant enzyme, and our observation of the lack of anion effects in the Mo^V EPR of the mutant enzyme supports the hypothesis that anions are reluctant to bind. These observations provide explanations for the observed nearly 2 orders of magnitude increase in K_m for R160Q relative to wild-type enzyme.[7,8]

According to simple Marcus theory[56] intramolecular electron-transfer rates depend on the reorganization energy, and changing this can slow electron transfer. Thus, for wild-type sulfite oxidase both reduced and oxidized enzymes are five-coordinate, and only bond-length changes upon electron transfer contribute to the reorganization energy. With R160Q SO, the fully reduced Mo^{IV} site is observed crystallographically to be five-coordinate,[13] and this is supported by our DFT calculations and consistent with our EXAFS measurements. Intramolecular electron-transfer rates have been measured using flash photoreduction of the cytochrome *b* with subsequent electron transfer to the oxidized Mo site, which is the opposite of the physiological direction. If the five-coordinate crystallographically observed structure for the R160Q SO Mo site is the same in solution, then electron transfer would involve dissociation of R160 from Mo which would in turn impact the reorganization energy and electron transfer.

In summary, we have shown that R160Q SO is coordinated by six ligands in the oxidized Mo^{VI} state and have used DFT calculations with constraints derived from the crystal structure to conclude that the molybdenum of the mutant enzyme is coordinated by Gln,[160] providing a molecular foundation for the kinetic incompetence of this mutant enzyme.

Acknowledgment. Portions of this work were carried out at the Stanford Synchrotron Radiation Laboratory which is funded by the Department of Energy Offices of Basic Energy Sciences and Biological and Environmental Research, with additional support from the National Institutes of Health, National Center for Research Resources. Work at the University of Saskatchewan was supported by a Canada Research Chair award (G.N.G.), the University of Saskatchewan, the Province of Saskatchewan, the Natural Sciences and Engineering Research Council, the National Institutes of Health, the Canadian Institute for Health Research, and the Canada Foundation for Innovation. Work at Duke University was supported by the National Institutes of Health (GM44283 and GM00091). The National Biomedical EPR Center is supported by the National Institutes of Health NIBIB EB001980.

Supporting Information Available: Tables of energy minimized coordinates for R160Q sulfite oxidase active sites in oxidized Mo^{VI} and reduced Mo^{IV} forms. This material is available free of charge via the Internet at http://pubs.acs.org.

JA071402A

(56) Gray, H. B.; Ellis, W. R., Jr. In *Bioinorganic Chemistry*; Bertini, I., Gray, H. B., Lippard, S. J., Valentine, J. S., Eds.; University Science Books: Mill Valley, CA, 1994; pp 315−363.